17th Australasian Fluid Mechanics Conference
Auckland, New Zealand
5-9 December 2010

Low Reynolds Number Bed Shear Stress Measurements Behind a Backward-facing Step Using PIV

M. Trevethan [1], J. E. Cater[2] and S. E. Coleman[1]

[1]Department of Civil and Environmental Engineering
The University of Auckland, Auckland 1142, New Zealand

[2]Department of Engineering Science
The University of Auckland, Auckland1142, New Zealand

Abstract

A series of experiments was carried out to investigate the bed shear stress distribution downstream of a backward-facing step. A viscous-fluid flume and a custom-made PIV system were used for the experiments of low Reynolds number flows to enable improved sampling resolutions for the near-bed flow. Reattachment lengths were found to match the indications of previous studies. If the hypothesis that the same process acts to generate sediment waves in laminar and turbulent flows is correct, then the present tests indicate that the bed shear stress distribution downstream of a bed perturbation does not lead to sediment-wave formation. Alternative aspects of boundary-layer redevelopment downstream of a bed perturbation are conjectured to lead to sediment-wave formation in nature.

Introduction

The generation from plane-bed conditions of sand waves on riverbeds is typically attributed to one of three phenomena: a) turbulent fluid motions, b) instability of the fluid-sediment flow system when perturbed, and c) granular transport mechanics. A wide spectrum of theories has been developed along these lines, with all of the theories still presenting unresolved inconsistencies [7].

In terms of potential wave generation due to granular motions, a number of investigations suggest that inception is via a scour-deposition wave arising with boundary-layer redevelopment downstream of a bed perturbation [17,23,24,26,21,29,7,8]. In this regard, flow development on the leeside of a bed perturbation of height s is found to give a maximum in the bed-stress distribution at a distance of $\lambda/s = O(30–40)$ downstream of the point of separation. With sediment transport a function of boundary shear stress, erosion and deposition will then occur upstream and downstream of this bed-stress maximum respectively, leading to generation of a second bed perturbation at this point, and successive wave generation downstream. The occurrence and location of the bed-stress maximum have been shown analytically [26], through numerical modelling [21], and through measurements in association with the occurrence of flow separation on the leeside of the bed perturbation [18,3]. The occurrence of such flow separation for small-amplitude bed perturbations is demonstrated by [29] and [30]. The rationale for the bed-stress maximum lies in the competing processes in this region of flow reacceleration acting to increase the bed stress and boundary-layer regrowth acting to decrease bed stress [26,12,21]. The former process is found to be dominant in the near field, with the latter process dominating in the far field. As conjectured by [26] and [31], the observed leeside bed-stress distribution could potentially also arise in the absence of separation (and thereby for smaller perturbation heights) simply through first-order adjustments in the velocity field downstream of a bed perturbation. The initial bed perturbation leading to boundary-layer redevelopment and wave generation could arise through several means, including a random sediment pileup, the impacts of turbulent events on the bed [30,14,2], or shear-wave interactions [13]. Coleman and Nikora [7,8] propose that such a bed disturbance arises through interactions of moving patches of sediment that result in a critical-height bed disturbance interrupting the bed-load layer. The initial moving sediment patches reflect the passage of sediment-transport events caused by attached eddies.

In order to further assess the possible linkage between sediment-wave formation and boundary-layer redevelopment downstream of a step, it was decided to undertake focused experiments to investigate the existence and streamwise location of a potential bed shear stress maximum behind a backward step. A viscous-fluid flume [5] was selected for the experiments to enable improved sampling resolution for the near-bed flow. Low Reynolds number flows could be adopted for the investigations owing to the conjecture that the mechanism of sediment-wave formation is the same for laminar and turbulent flows [6,7,20].

Numerous investigations of boundary-layer redevelopment downstream of a step have been carried out previously, with [10] summarising results to that point of time concerning the effects on flow development on the leeside of a step of: initial boundary-layer state and thickness, free-stream turbulence, pressure gradient, and aspect ratio. Studies to date, however, predominantly a) focus on a shortened region immediately downstream of the step [11,15, 27], and/or b) utilise wind tunnels [3,10,1,16,19,15] or closed-conduit water tunnels [9,27,28,22]. In contrast to the earlier studies, this investigation involves open-channel liquid (oil) flows, where [11] used open-channel water flows, and investigates up to 210 step heights downstream of the step.

Experimental Investigations

The experiments were conducted in a glass-sided tilting open-channel flume measuring 10 m x 0.4 m (wide), with a maximum fluid depth of 0.2m (figure 1). A tank measuring 1.5m long, 0.65m wide and 1.6m deep collects fluid at the downstream end of the open-channel section. A twin-screw positive-displacement pump returns the fluid from the tank via a 250mm diameter pipe to the top end of the flume, where it passes through a 515mm

long flow-straightening grid of 50x57mm openings. In order to reduce air bubble entrainment in the collection tank, where the accumulating bubbles would be detrimental to flow measurements, a series of vanes had been installed (running parallel to the flow) in the tank to create drag and reduce flow velocity. A double-cup-shaped curved section installed at the downstream end of the vanes acts to turn the flow away from the end wall and back down the sides of the tank, where it is separated from the incoming flow by the outer guide vanes. The step tested in the present experiments comprised a 2.33m long 15mm thick Perspex sheet that extended across the flume width. The step and flume bed surfaces were hydraulically smooth.

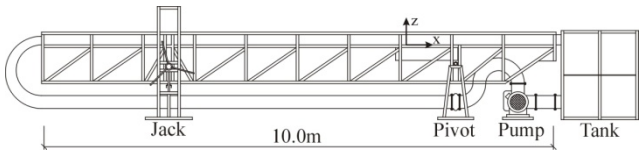

Figure 1. Viscous-fluid flume.

The oil used was Shell Ondina 15, a white mineral oil with a density of ρ = 850 kg/m^3 and a kinematic viscosity of 34×10^{-6} m^2/s at 20^{o}C. More generally, the kinematic viscosity of the oil can be described by ν (m^2/s x 10^{-6}) = $-8.333\times10^{-4}T^3 + 0.100T^2 - 4.617T + 93.00$ for oil temperatures of T = 10-40^{o}C [4]. The characteristics of the three principal flows tested, E1T1, E1T2 and E1T3, are given in table 1, where h, U and u_* are depth, depth-averaged velocity, and shear velocity for the approach flow on the step. R_s = Us/ν and R_h = Uh/ν are Reynolds numbers based on the step height and flow depth, respectively, where s is the step height.

Test	s (m)	T (^{o}C)	h (m)	U (m/s)	u_* (m/s)	R_s	R_h
E1T3	0.015	21	0.1065	0.1294	0.0122	60	425
E1T1	0.015	22	0.1040	0.2491	0.0169	121	837
E1T2	0.015	23	0.1040	0.4946	0.0249	251	1740
E1T1tri	0.016	20.5	0.1180	0.2105	0.0145	101	748
E1T1nsm	0	20	0.1380	0.2179	0.0164	0	885

Table 1. Characteristics of the tested flows.

Flow measurements were made using the Particle Image Velocimetry (PIV) measuring system developed at the University of Auckland [25]. This system uses the scanning beam technique to capture 200 PIV images per second, the present investigations measuring a 120x120mm plane at a resolution of 960x960 pixels. For each test, measurements were made along the flume centreline at successive 100mm distances behind the step by moving the step upstream from a fixed flow measurement position (located 8m downstream of the flume entrance). Overlapping the measurement regions allowed the output vectors at the upstream and downstream edges of successive regions to be discarded. A 5 second sample was collected at each step position.

The lightsheet for the PIV system is generated from a 5W CW 532 nm Nd:YVO4 laser using a galvanometer-driven mirror (computer controlled) together with a parabolic mirror. The system has several advantages over rotating-polygon type scanning systems, including: that the mirror is always positioned at the focal point of the parabola, and that the lightsheet generation is extremely versatile, with the lightsheet width (for a single parabolic mirror) and beam scan velocities easily and independently adjustable. Additionally, the beam scan velocity, which is typically nonlinear in rotating-polygon systems due to inherent properties of parabolic reflectors, can be constant in a galvanometer-based system (giving a uniform intensity lightsheet) by driving the galvanometer at an unsteady angular velocity. Integrated synchronisation options for the system permit frame-straddling techniques to be used in order to reduce interframe times for the high-speed camera to below 1/(camera frame rate). The system as designed is capable of resolving flow fields at frequencies of up to 200 Hz (covering the typical scales of interest for hydraulic researchers), with recording durations of over 8 min.

The output PIV data for the present tests comprised velocity vector information at a frequency of 200 Hz and spatial resolutions of 1 mm vertically and horizontally. The double-averaged (in time and space) streamwise velocity distribution $\langle\bar{u}\rangle(z)$ was calculated for the approach flow above the step, from which the depth-averaged velocity U, shear velocity u_*, and flow Reynolds numbers were calculated (table 1). The time-averaged bed shear stress $\bar{\tau}$ at each position along the channel was calculated using $\bar{\tau} = \mu(d\bar{u}/dz)$, where $\bar{u}$ = time-averaged longitudinal velocity; z = vertical position; and μ = dynamic viscosity. Due to lower quality data immediately adjacent to the bed, for each position across the PIV sheet, the velocity gradient $(d\bar{u}/dz)$ was determined using a two-point linear fit to the time-averaged velocity data collected at 2mm and 6mm above the bed. The bed shear stress variation behind the backward facing step for each test was then plotted as $\bar{\tau}(x)$, where x is distance in the streamwise direction (figure 1). The laminar-transitional natures of the principal tested flows are reflected in the R_h values given in table 1, and also the figure 2 measured velocity distributions for the approach flows.

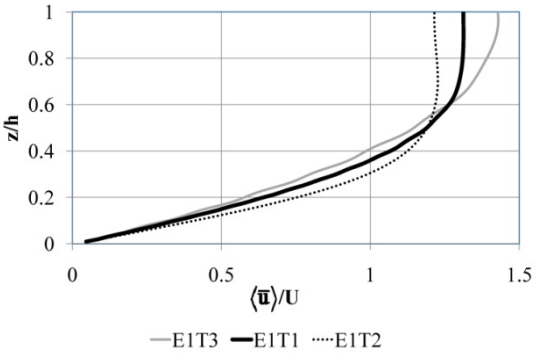

Figure 2. Normalised approach-flow velocity distributions.

Boundary-layer Redevelopment

Figure 3 shows the variation of normalised time-averaged bed shear stress with distance behind the backward-facing step for the three principal tests E1T3, E1T1, and E1T2.

For these low Reynolds number tests, the bed shear stress does not show a clear peak within the present measurement region extending to 220 step heights downstream from the step. These results appear to be different to earlier bed shear stress measurements behind backward facing steps conducted in closed conduits and under more turbulent flow conditions [18,3]. These results are also different to expectations based on the hypothesis that a boundary shear stress peak downstream of a bed disturbance causes bedform generation in the same way for both laminar and turbulent flows. If the same process acts to generate seed waves in laminar and turbulent flows [6], then the results of

figure 3 suggest that the cause does not lie in the shape of the bed shear stress distribution. These seed waves may simply arise through first-order adjustments in the velocity field (and thereby bed pressures) downstream of a bed perturbation as conjectured by [26] and [31].

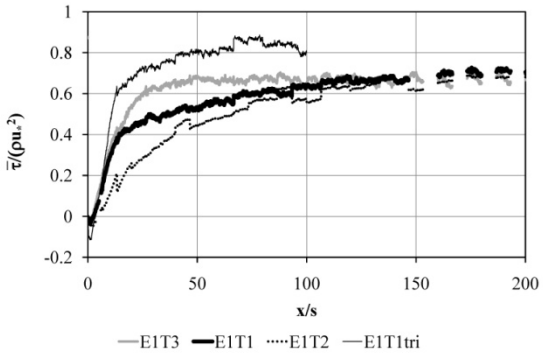

Figure 3. Normalised time-averaged bed shear stress distributions downstream of a backward-facing step.

Figure 4 shows the normalised bed shear stress distribution immediately downstream of the step for the principal tests E1T3, E1T1, and E1T2. Defining the reattachment length by the position of zero bed stress [19,15,22], figure 4 indicates reattachment lengths of approximately 2-5 step heights for the tests of R_s = 60-250 (table 1). [9] and [22] indicate expected reattachment lengths of approximately 3-10 step heights over this range of R_s, consistent with the indications of figure 4, particularly where [1] report a decrease in reattachment length with decreasing expansion ratio at a constant Reynolds number, and the expansion ratios for the present tests are [(h+s)/h] = 1.14.

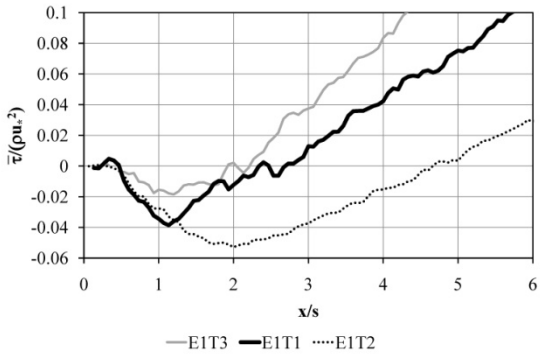

Figure 4. Normalised time-averaged bed shear stress distributions immediately downstream of the step.

In order to consider the effect on the leeside bed shear stress distribution of a short near-bed perturbation, test E1T1 was repeated as E1T1tri using a triangular prism extending across the flume in lieu of the long step. The symmetrical prism measured 16mm high, with a base length of 20mm. The characteristics of the approach flow for test E1T1tri are given in table 1. The measured bed shear stress distribution given in figure 3 for test E1T1tri is similar to that obtained for the long step of E1T1, and again shows no clear evidence of a peak within 100 step heights downstream of the prism (particularly where $\overline{\tau}/\left(\rho u_*^2\right)=1$ is expected for large x/s).

Further experiments are planned to investigate the effect of a roughened bed on the bed shear stress distribution downstream of the step.

Flow Layering

An interesting result of the present tests was the evidence of bands in contour plots of the standard deviation of longitudinal velocity σ_u for the tests of low Reynolds numbers (figure 5). For test E1T2 of larger Reynolds numbers, any such bands were less extensive and more subtle. In order to test whether this banding arose due to either the flow straightening grid at the upstream end of the flume or the acceleration of flow up onto the step in the flume bed, the step was removed to give a smooth planar bed, and the grid was replaced with a thin perforated sheet of closely-spaced 2mm diameter openings. Test E1T1 was then repeated as test E1T1nsm (table 1). Figure 5c shows that the banding still occurred for the change of inlet conditions. Trials also confirmed that the data processing did not introduce the banding apparent in figure 5. Spectral analysis of velocity time series in the high and low variance bands downstream of the step for test E1T1 showed a uniform increase in spectral energy across all frequencies greater than 1Hz for the high-variance band. The bands for the low Reynolds number flows were concluded to be physically valid, and are not expected to influence the bed shear stress findings of the study.

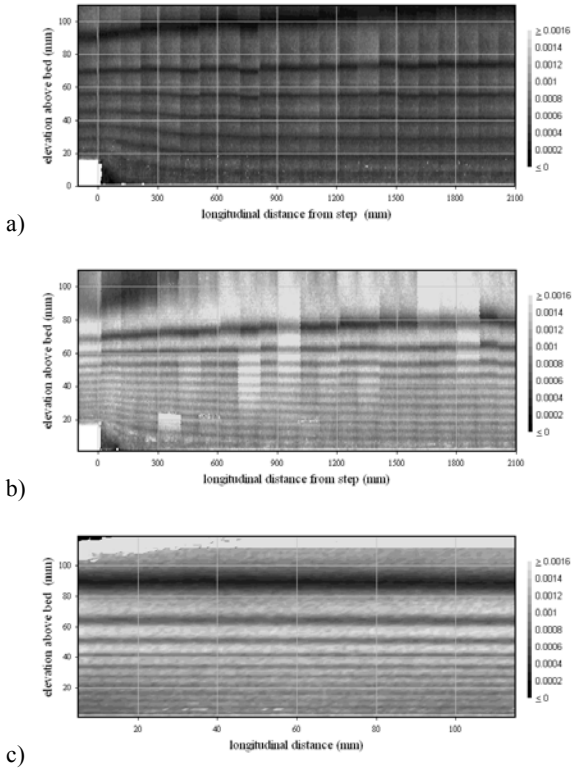

a)

b)

c)

Figure 5. Contours of σ_u: a) E1T3; b) E1T1; and c) E1T1nsm.

Conclusions

Measurements of bed shear stress distributions downstream of a backward-facing step were made using PIV for low Reynolds number flows. Reattachment lengths were found to be consistent with the findings of [9] and [22]. In contrast to previous measurements behind backward facing steps conducted in closed conduits and under more turbulent flow conditions, the bed shear stress does not show a clear peak (within 220 step heights) downstream of the step for the present low Reynolds number

tests. If the same process acts to generate seed waves in laminar and turbulent flows [6], then the present results suggest that the cause does not lie in the shape of the bed shear stress distribution. As conjectured by [26] and [31], these seed waves may alternatively simply arise through first-order adjustments in the velocity field (and thereby bed pressures) downstream of a bed perturbation.

References

[1] Armaly, B.F., Durst, F., Pereira, J.C.F. & Schönung, B., Experimental and Theoretical Investigation of Backward-Facing Step Flow, *J . Fluid Mech.*, **127**, 1983, 473-496.

[2] Best, J.L., On the Entrainment of Sediment and Initiation of Bed Defects: Insights from Recent Development Within Turbulent Boundary Layer Research, *Sedimentology*, **39**, 1992, 797– 811.

[3] Bradshaw, P. & Wong, F.Y.F., The Reattachment and Relaxation of a Turbulent Shear Layer, *J. Fluid Mech.*, **52**, 1972, 113-135.

[4] Cameron, S.M., Near-boundary Flow Structure and Particle Entrainment, PhD thesis, The University of Auckland, Auckland, New Zealand, 2006.

[5] Cameron, S.M., Coleman, S.E., Melville, B.W. & Nikora V.I., Marbles in Oil, Just Like a River?, in *River Flow 2006*: International Conference on Fluvial Hydraulics, editors R.M.L. Ferreira et al., Taylor and Francis, Philadelphia, Pa., 2006, 927–935.

[6] Coleman, S.E. & Eling, B., Sand Wavelets in Laminar Open-channel Flows, *J. Hyd. Res.*, IAHR, **38(5)**, 2000, 331-338.

[7] Coleman, S.E. & Nikora, V.I., Bed and Flow Dynamics Leading to Sediment-wave Initiation, *Water Resources Research*, **45** W04402, doi:10.1029/2007WR006741, 2009.

[8] Coleman, S.E. & Nikora, V.I., Fluvial Dunes: Initiation, Characterisation, Flow Structure, accepted for publication in *Earth Surface Processes and Landforms*, 2011.

[9] Denham, M.K. & Patrick, M.A., Laminar Flow over a Downstream-facing Step in a Two-dimensional Flow Channel, *Trans. Instn. Chem. Engrs.*, **52**, 1974, 361-367.

[10] Eaton, J.K. & Johnston, J.P., A Review of Research on Subsonic Turbulent Flow Reattachment, *AIAA J.*, **19**, 1981, 1093-1100.

[11] Etheridge, D.W. & Kemp, P.H., Measurements of Turbulent Flow Downstream of a Rearward-facing Step, *J. Fluid Mech.*, **86**, 1978, 545-566.

[12] Fredsøe, J., Shape and Dimensions of Stationary Dunes in Rivers, *J. Hyd. Div.*, ASCE, **108(8)**, 1982, 932–947.

[13] Gyr, A. & Kinzelbach, W., Bed Forms in Turbulent Channel Flow, *Appl. Mech. Rev.*, **57(1)**, 2004, 77-93.

[14] Gyr, A. & Schmid, A., The Different Ripple Formation Mechanism, *J. Hyd. Res.*, **27(1)**, 1989, 61- 74.

[15] Hancock, P.E., Low Reynolds Number Two-dimensional Separated and Reattaching Turbulent Shear Flow, *J. Fluid Mech.*, **410**, 2000, 101-122.

[16] Hasan, M.A.Z., The Flow over a Backward-facing Step Under Controlled Perturbation: Laminar Separation, *J. Fluid Mech.*, **238**, 1992, 73-96.

[17] Inglis, CC., *The Behaviour and Control of Rivers and Canals (With the Aid of Models)*, Res. Publ. 13, Central Waterpower lrrigation and Navigation Research Station, Poona, India, 1949.

[18] Jones, D.F., An Experimental Study of the Distribution of Boundary Shear Stress and its Influence on Dune Formation and Growth, MSc thesis, University of Washington, Seattle, WA, 1968.

[19] Jović, S., Recovery of Reattached Turbulent Shear Layers, *Experimental Thermal and Fluid Science*, **17**, 1998, 57-62.

[20] Lajeunesse, E., Malverti, L., Lancien, P., Armstrong, L., Metivier, F., Coleman, S., Smith, C.E., Davies, T., Cantelli, A. & Parker, G., Fluvial and Subaqueous Morphodynamics of Laminar and Near-laminar Flows: a Synthesis, *Sedimentology*, **57**, 2010, 1–26.

[21] McLean, S.R. & Smith, J.D., A Model for Flow over Two-dimensional Bed Forms, *J. Hyd. Engrg.*, ASCE, **112**, 1986, 300-317.

[22] Mouza, A.A., Pantzali, M.N., Paras, S.V. & Tihon, J., Experimental and Numerical Study of Backward-facing Step Flow, *5th National Chemical Engineering Conference*, Thessaloniki, Greece, 2005, 4pp.

[23] Raudkivi, A.J., Study of Sediment Ripple Formation, *J. Hyd. Div.*, ASCE, **89(HY6)**, 1963, 15–33.

[24] Raudkivi, A.J., Bed Forms in Alluvial Channels, *J. Fluid Mech.*, **26(3)**, 1966, 507-514.

[25] Schlicke, T., Cameron, S.M. & Coleman, S.E., Galvanometer-based PIV for Liquid Flows, *Flow Measurement and Instrumentation*, **18**, 2007, 27–36.

[26] Smith, J.D., Stability of a Sand Bed Subjected to a Shear Flow of Low Froude Number, *J. Geophys. Res.*, **75(30)**, 1970, 5928-5940.

[27] Tihon, J., Legrand, J. & Legentilhomme, P., Near-wall Investigation of Backward-facing Step Flows, *Experiments in Fluids*, **31**, 2001, 484-493.

[28] Tylli, N., Kaiktsis, L. & Ineichen, B., Sidewall Effects in Flow Over a Backward-facing Step: Experiments and Numerical Simulations, *Physics of Fluids*, **14(11)**, 2002, 3835-3845.

[29] Venditti, J.G., Church, M.A. & Bennett, S.J., Bed Form Initiation from a Flat Sand Bed, *J. Geophys. Res.*, **110**, F01009 DOI:10.1029/2004JF000149, 2005.

[30] Williams, P.B. & Kemp, P.H. Initiation of Ripples on Flat Sediment Beds, *J. Hyd. Div.*, ASCE, **97(4)**, 1971, 505–522.

[31] Yalin, M.S., *River Mechanics*, Pergamon Press, Inc., New York, N.Y., U.S.A, 1992.